Mansoura Engineering Journal

Volume 29 | Issue 1 Article 14

12-27-2020

Matching of PV Power Systems with Electrical Loads Using Graph Theoretic Modeling Approach.

Magdy Mohamed El-Saadawi
Electrical Power & Machines Department., Faculty of Engineering., El-Mansoura University., Mansoura., Egypt

Mohamed Adel El-Sayes
Electrical Power & Machines Department., Faculty of Engineering,El- Mansoura University., Mansoura., Egypt

M. Abdel-Wahab
Egyptian Elect. Holding Company Zagazig., Egypt

Recommended Citation

El-Saadawi, Magdy Mohamed; El-Sayes, Mohamed Adel; and Abdel-Wahab, M. (2020) "Matching of PV Power Systems with Electrical Loads Using Graph Theoretic Modeling Approach.," *Mansoura Engineering Journal*: Vol. 29 : Iss. 1 , Article 14.
Available at: https://doi.org/10.21608/bfemu.2020.132708

MATCHING OF PV POWER SYSTEMS WITH ELECTRICAL LOADS USING GRAPH THEORETIC MODELING APPROACH

مواءمة نظم القوى الشمسية الفوتوفولتية مع الأحمال الكهربية باستخدام طريقة نمذجة المخططات النظرية

M. M. EL-SAADAWI M. A. EL-SAYES M. N. ABDEL-WAHAB

Electrical Power & Machines Dept., Faculty of Engineering, Mansoura University.

Egyptian Elect. Holding Company Zagazig

خلاصة:

تعتبر المواءمة بين الخلايا الفوتوفولتية والأحمال الكهربية التى تغذيها من أهم العوامل التى تؤثر فى كفاءة أداء المنظومة الفوتوفولتية والاستفادة القصوى من الطاقة الناتجة عن الخلايا. وفى حالة المواءمة الجيدة بين الخلايا والأحمال يكون منحنى التحميل قريبا من منحنى القدرة القوى الناتجة عن الخلايا عند قيم إشعاع مختلفة.

ويقدم هذا البحث طريقة جديدة لمواءمة نظام شمسي مكون من منظومة خلايا فوتوفولتية مستقلة تغذى حمل ميكانيكي من خلال محرك تيار مستمر. وقد تم استنباط وتطوير برنامج كومبيوتر بلغة MATLAB 6 لتمثيل المكونات المختلفة للنظام بطريقة نمذجة المخططات النظرية. ومن ثم تطبيق هذا البرنامج على عدد من دراسات الحالة لأنواع مختلفة من محركات التيار المستمر والأحمال الميكانيكية والمقارنة بينها للوصول إلى أفضل مواءمة بين الخلايا وكل نوع من أنواع الأحمال.

ABSTRACT

The quality of load matching in a photovoltaic power system (PVPS) determines the system performance and the degree or the solar cells utilization. In a good matched system, the operation of the load–line is close to the maximum power–line of the solar cell (SCA) generator. This paper presents a new methodology for modeling a stand alone PVPS using the Graph Theoretic Modeling (GTM) Approach. The studied system composed of a directly connected SCA generator-dc motor supplying different load types. A computer program (written in MATLAB 6) has been developed to model the studied system. The computer program is then applied to nine case studies for different types of dc-motors and various mechanical loads. A comparison between these cases is introduced to indicate the appropriate motor type for each load.

1. INTRODUCTION

The quality of load matching in a photovoltaic power system (PVPS) determines the system performance and the degree or the solar cells utilization. In a good matched system, the operation of the load–line is close to the maximum power–line of the solar cell (SCA) generator. Computer simulation for the operation and sizing of photovoltaic (PV) components is a very thorough method of determining the behavior of PVPS. Using simulation methods the electrical power output can be optimized with respect to component sizes. A method of detailed modeling and simulation must be available before the issue of optimum sizing is adequately pursued. The topics of modeling and simulating PV powered systems which, include PV array, DC motor and mechanical load was well documented in [1], [2], and [3]. An investigation of directly coupled photovoltaic pumping connected to a large absorber field through modeling and simulating PV array, dc motor,

Accepted February 16, 2004.

centrifugal pump and the absorber field was presented in [4]. Detailed modelings of Photovoltaic system components using TRANSYS program were analyzed in [5]. Whereas, Ref. [6] applied the TRNSYS program to a large scale PVPS used for water heating and expanded the model to add more components to the program. Ref [7] investigated the long-term performance of PV pumping system with a maximum power point tracker. The operation characteristics of dc-permanent, series motor and shunt motor with a centrifugal load was presented and compared in [8]. A mathematical methodology for the optimum configuration of photovoltaic pumping system in a solar domestic hot water was investigated in [9]. One of the widely accepted network theories is the Graph Theoretic Modeling (GTM) Approach. The GTM approach has been in use since 1955. It has emerged as a method that allows the modeling and solving of systems that are hydraulic, pneumatic, structural, mechanical and thermal or combination thereof [10]. A method for modeling the directly-connected stand-alone PVPS using GTM method was introduced in Ref. [11]. The paper presented an approach to reduce the computational efforts needed in setting up the required equations. The GTM approach was applied to a PV powered ventilator system and a PV powered pumping system [11].

This paper applies a comprehensive study of applying the GTM approach to a directly connected SCA generator to supply different load type. The load may be constant, ventilator or centrifugal pump. Whereas, the used dc motor may be series, separately excited or shunt motor. The system components are modeling using GTM approach to generate a nonlinear system of equations called Newton-Raphson Mixed Nodal Tableau (NR-MNT). The equations are then solved numerically by developing a computer program written in MATLAB 6. A comparison between the different case studies is achieved based on the quality of load matching for each case.

2- SOLVING NONLINEAR SYSTEMS USING GTM APPROACH

The GTM approach provides a set of equations that characterize the individual components of the system. The component is the smallest indivisible element of our interest within a system. The behavior of a component can be characterized by using two types of variables [11]:

- ***Through variables (y)***: quantify flow process such as current, torque and flow rate.
- ***Across variables (x)***: quantify the stimulus causing flow such as voltage, speed and hydraulic head.

For modeling a combined PV-dc motor system, components of electrical, mechanical and hydraulic are encountered. When the components are replaced by their terminal graphs, the resulting diagram is called ***system graph***. The system graph depicts the connectivity of components without any ambiguity. The system graph can be easily converted into a matrix form ***(incident matrix)*** to indicate the connectivity of the system components. The incident matrix performs this task through the use of +1, -1&0's. Rows and columns represent the individual nodes and edges, respectively. With the help of the incident matrix both the ***vertex*** and the ***nodal transformation*** equations are evolved. The vertex equations stem from a generalization of Kirchoff's current law (to incorporate systems other than electrical networks). This matrix ensures the conservation of flow at each node and appears as:

$$\begin{bmatrix} A_a & A_c & A_r & A_t \end{bmatrix} \begin{bmatrix} Y_a \\ Y_c \\ Y_r \\ Y_t \end{bmatrix} = [0] \tag{1}$$

Where: A_a and A_r, are across and variable sources respectively. A_c and A_r, are conductive and resistive portions of constitutive components respectively. The vectors with Y represent the set of all the through variables y partitioned analogous to the incidence matrix A corresponding to the component types. The nodal transformation equations provide the relationship between component across variables (X_a , X_c , X_r , X_t) to the nodal across variables (X_n). The vectors with X represent the collection of across variables X partitioned analogous to the incidence matrix A corresponding to the component type.

$$\begin{bmatrix} X_a \\ X_c \\ X_r \\ X_t \end{bmatrix} = \begin{bmatrix} A_a^T \\ A_c^T \\ A_r^T \\ A_t^T \end{bmatrix} * X_n \tag{2}$$

These two sets of equations give rise to a system of equation known as ***Mixed Nodal Tableau (MNT)*** [11]. The MNT system of equations is formulated to find a set of variables that once solved, is sufficient to calculate all other system variables. For linear systems the MNT is a system of equations summarizing the behavior of the system. For nonlinear systems the same set of equations is used to formulate the ***Newton Raphson Mixed Nodal Tableau (NR MNT)***, which have to be solved iteratively, explained later.
Expanding Eq. (1) and substituting for Y_c with the conductive vector G_c , the vertex equation can be rewritten as:

$$A_a Y_a + A_c G_c + A_r Y_r + A_t Y_t = 0 \tag{3}$$

Where the values of through sources Y_t are known. Using the identity for X_c in Eq. (2), and substituting X_r for the resistive vector P_r, the following can be written as :

$$A_r^T X_n - P_r = 0 \tag{4}$$

By using the identity of X_a from Eq.(3), a third set of equations using a generalization of Kirchoff's voltage law, can be written as:

$$A_a^T X_n - Xa = 0 \tag{5}$$

Where the values of the across sources X_a are known. Equations (3)-(5) can consolidated and designated as the MNT F(z) which represent a set of nonlinear equations in which there are the same number of unknown variables $Z^T = [\, X_n^T \;\; Y_r^T \;\; Y_a^T \,]$ as the number of equations:

$$[F(z)] = \begin{bmatrix} f_1(z) \\ f_2(z) \\ f_3(z) \end{bmatrix} = \begin{bmatrix} A_c G_c + A_r Y_r + A_a Y_a + A_t Y_t \\ A_r^T X_n - P_r \\ A_a^T X_n - X_a \end{bmatrix} \tag{6}$$

The Newton–Raphson method is used to solve this system of non linear equations as follows:

$$\left. \frac{\partial F(z)}{\partial z^T} \right|_{z=z^k} \Delta z^{k+1} = -F(z)\Big|_{z=z^k} \tag{7}$$

where Δz^{k+1} is given by $(z^{k+1} - \Delta z^k)$ in which z^k is the k $\underline{th}$ iterative guess for z . The Jacobian can be written as:

$$F^{1z} = \frac{\partial F(z)}{\partial z^T} = J\{F(z)\} = \begin{bmatrix} \frac{\partial f_1(z)}{\partial X_n^T} & \frac{\partial f_1(z)}{\partial Y_r^T} & \frac{\partial f_1(z)}{\partial Y_a^T} \\ \frac{\partial f_2(z)}{\partial X_n^T} & \frac{\partial f_2(z)}{\partial Y_r^T} & \frac{\partial f_2(z)}{\partial Y_a^T} \\ \frac{\partial f_3(z)}{\partial X_n^T} & \frac{\partial f_3(z)}{\partial Y_r^T} & \frac{\partial f_3(z)}{\partial Y_a^T} \end{bmatrix} \tag{8}$$

Where F^{1z} is a notation for the first order partial derivative of the MNT equations $F(z)$ with respect to the transpose of the vector z.
Throughout this paper a similar notation is used in which a^{1b} is the first order partial derivative of a with respect the transpose of vector b. Using this notation (7) can be expanded and written as:

$$F^{1z}\Big|_{z=z^k} z_{k+1} = -F(z)\Big|_{z=z^k} + F^{1z}\Big|_{z=z^k} z_k \tag{9}$$

By performing the operation indicated in Eq. (9) on Eq. (6), the NR MNT system of equations is found as:

$$\begin{bmatrix} A_c G_c^{1X_c} A_c^T & A_c G_c^{1Y_r} + A_r & A_a \\ A_r^T - P_r^{1X_c} A_c^T & -P_r^{1Y_r} & 0 \\ A_a^T & 0 & 0 \end{bmatrix}_{\substack{X_c = A_c^T X_n^k \\ Y_r = Y_r^k}} \begin{bmatrix} X_n^{k+1} \\ Y_r^{k+1} \\ Y_a^{k+1} \end{bmatrix} =$$

$$\begin{bmatrix} -A_c G_c + A_c G_c^{1X_c} A_c^T X_n + A_c G_c^{1Y_r} Y_r - A_t Y_t \\ P_r - P_r^{1X_c} A_c^T X_n - P_r^{1Y_r} Y_r \\ X_a \end{bmatrix}_{\substack{X_c = A_c^T X_n^k \\ Y_r = Y_r^k}} \tag{10}$$

Where [NR MNT] or [NR R] is used, it refers to the left side matrix and the right side vector, respectively. When NR MNT is mentioned, it refers to the entire system of equations.
Eq. (10) can be solved iteratively by evaluating:

$$\begin{bmatrix} X_n^{k+1} \\ Y_r^{k+1} \\ Y_a^{k+1} \end{bmatrix} = [\text{NR MNT}]^{-1}[\text{NR R}] \tag{11}$$

3- APPLYING THE GTM APPROACH TO COMBINED PV-DC MOTOR SYSTEMS

Any system consists of different components; each component has its behavior and its special characteristics that can be replaced by a stamp on behalf this component. By modeling any component using the GTM approach we can create a stamp of each one by identifying the following items:

- Schematic diagram,
- Component type,
- System terminal graph,

- System incident matrix,
- System terminal equation,
- Newton Raphson Mixed Nodal Tableau [NR MNT] and
- Newton Raphson Reduction [NR R].

3-1 Steps of Applying GTM Approach to a System

In this paper we will apply the GTM approach to a combine PV-dc motor system supplying different mechanical load types to obtain the optimum utilization of solar radiation. Following are the main steps required to apply the GTM approach on any system:

1. ***Draw the terminal graph of the system.***
   - The "component terminal graph" represents the combination of all edges (line segments) and nodes (end points of edges) associated with a single component are drawn. The components are then replaced by terminal graph, and the resulting diagram of nodes and edges express "system graph".
   - The "incident matrix" is formulated using the system graph, which depicts the connectivity of components without any ambiguity.
   - The nodes are designated by letters and the edges are designated by numbers.
2. ***Identify the system terminal equations.***
   - The across and through variables mathematical relations for each component are expressed.
   - The number of terminal equations of the system is equal to the dimension of "NRMNT" matrix.
   - "Across variables" denotes the stimulus causing flow such as (V,H,ω)
   - "Through variables" denotes flow process such as (I,Q,T).
3. ***Create incident matrix:***
   - The incident matrix connects the system components through the use of +1, -1, and 0s. The individual a_{ij} th element of the incident matrix A is given a value as follows:

$$a_{ij} = \begin{Bmatrix} 0 \\ 1 \\ -1 \end{Bmatrix} \textit{ if the j th edge is } \begin{Bmatrix} \textit{not incident on} \\ \textit{incident and towards} \\ \textit{incident on and away from} \end{Bmatrix} \textit{ the i th node}$$

   - If the component does not exist, the corresponding sub-matrix altogether is omitted from the matrix; the datum nodes are omitted from the matrix because they offer redundant information.

$$A = [\, A_a \;\; A_c \;\; A_r \;\; A_t \,]$$

4. ***Get the variables***

The variables include the across, through, and nodal across variables:

Across variables $[\, X_a : X_c : X_r (P_r) : X_t \,]$

Through variables $[\, Y_a : Y_c (g_c) : y_r : y_t \,]$

Nodal across variable $[X_n]$

Where

(X_a, Y_a) complementary pair associated each other, (X_a) presents across source such as voltage source and static head [V_{in}], [H_{static}], (Y_a) complement pair of [X_a].

(X_c, Y_c) (Y_c) conductive portion of constitutive component (motor or pump) such as: current, torque and flow rate related to the motor or the pump, (X_c) often not included.

(P_r, Y_r) (P_r) resistive portion of constitutive component such as the input voltage of a motor or the input speed of a pump, (Y_r) complement pair array of (P_r).

$(X_t ; Y_t)$ (Y_t) through sources such as current source (I_{ph}) or constant torque source (T_{const}) (X_t) complement pair of (Y_t) not included across variable (X_n) at each node such as (V_a; ω_h ; H).

5. *Formulate the [NR MNT] and [NR R]*

Use the system equations and the variables of the system to substitute in the Jacobean matrix Eq. (8) to get the [NR MNT], then substitute in Eq. (9) to get Newton Raphson Reduction [NR R].

6. *Numerically Solve the problem*

The [NR MNT] and [NR R] are solved numerically by developing a MATLAB computer program to get the sufficient parameters to characterize the system (V, I, T, ω, H, Q). These parameters are then used to compute the electrical output power of SCA generator (P_{elect}), the mechanical output power of the dc motors (P_{mech}), the hydraulic power of the pump (P_{hyd}), and the system efficiency (η) and utilization (μ) as we will explain in the following sections.

3-2 Modeling of Combined PV-DC Motor Systems Using GTM Approach

Load types may be connected to the SCA generator–dc motor combination according to the required application .The main purpose of this paper is to indicate the quality of load matching for different mechanical load types connected to dc motors and powered by SCA generator for optimum utilization of solar radiation using (GTM) technique. The dc motors can be classified, according to the type of field excitation, into: series, permanent magnet, shunt and separately excited motors. Permanent magnet motors have similar equations as separately excited ones in case of constant field current. The widely used mechanical load types can be categorized as: constant load, ventilator load and centrifugal pump. The following section will analyze each of the three load connected to different motor types to compromise suitable matching. The results are used to compare between different case studies.

3-2-1 SCA generator modeling

The SCA generator can be modeled as a current source in parallel to a diode. Series resistance (R_s) accounts for the total resistance at the PV cell/wire contact interface as shown in Fig. 1-a. The current through the diode can be expressed as:

$$I_1 = I_o(e^{V_1/\sigma} - 1) \tag{13}$$

Where: $\sigma = KT/q$

σ : Thermal voltage, 1/volt

K : Botzman constant

T : Absolute temperature in Kelvin

q : Electron charge, Coulomb

I_o : Reverse Saturation current, A

The current through the series resistance is $I_2 = V_2 / R_s$ as shown in Fig. 1-a.

3-2-2 Terminal equations of dc motors

The (GTM) methodology deals with the motor as a 4-terminal constitutive component due to the transuding nature of the motor which, converts electrical energy to mechanical energy. The input of the motor is the voltage gained from SCA should be in resistive form i.e. $[P_r]=[V_3]$ whereas, the output of the motor (the electromagnetic torque delivered to the load) should be in conductive form i.e. $[G_c] = [T_4]$. The subscript (3) and (4) denotes to voltage and torque edges. The voltage and torque equations representing the dc motors can be drawn as [8]:

i) Series motors

$$V_3 = M_{af} I_3 \omega_4 + R_a I_3$$
$$T_4 = -M_{af} I_3^2 + B\omega_4 \quad (14)$$

ii) Separately exited motors

$$V_3 = c_e \omega_4 + R_a I_3$$
$$T_4 = -c_e I_3 + B\omega_4 \quad (15)$$

iii) Shunt motors

$$V_3 = \left(\frac{R_a R_f}{R_a + R_f - M_{af}\omega_4}\right) I_3$$
$$T_4 = \left(\frac{M_{af}(R_f - M_{af}\omega_4)}{R_a}\right)\left(\frac{R_a}{R_a + R_f - M_{af}\omega_4}\right)^2 I_3^2 \quad (16)$$

Where

I_3 , V_3 : Motor input current and voltage (at edge 3),
R_a , R_f : Armature and field resistances of the dc motor, Ω
M_{af} : Mutual inductance between armature and field, H
B : Viscous Torque constant of rotational losses, N.m /rad/s
C_e : Flux coefficient, V/rad/sec
ω_4 , T_4 : Motor output speed and torque (at edge 4),

3-2-3 Modeling of different load types

a) Constant Load Torque

In steady state operation, the electromagnetic torque value is the summation of the constant load torque plus mechanical losses so that: T_l = constant. The schematic diagram of the constant load torque and the system graph is shown in Fig 1-a, 1-b.

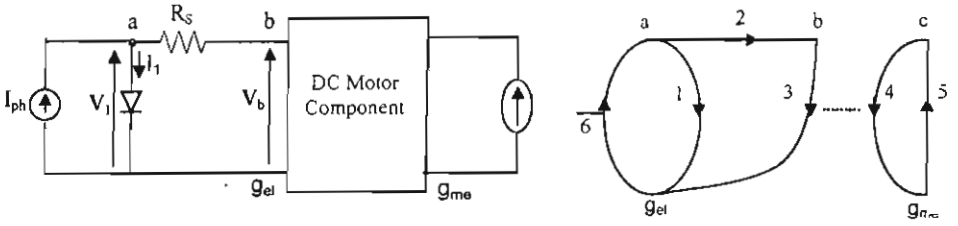

a- Schematic diagram b- System graph

Fig. 1 Schematic diagram and system graph of constant load powered by SCA generator

The ***incident matrix*** of this system is:

$$A = \begin{array}{c} \\ a \\ b \\ c \end{array} \begin{array}{c} \begin{array}{cccccc} A_c & & & A_r & & A_t \end{array} \\ \begin{array}{cccccc} 1 & 2 & 4 & 3 & 5 & 6 \end{array} \\ \left[\begin{array}{cccccc} 1 & 1 & 0 & 0 & 0 & -1 \\ 0 & -1 & 0 & 1 & 0 & 0 \\ 0 & 0 & 1 & 0 & -1 & 0 \end{array}\right] \end{array}$$

The ***variables*** required to solve the NRT MN system of equations are:

$$P_r = [V_3] \;;\; G_c = \begin{bmatrix} I_1 \\ I_2 \\ T_4 \end{bmatrix} \;;\; X_n = \begin{bmatrix} V_a \\ V_b \\ \omega_c \end{bmatrix} \;;\; y_r = [I_3] \;;\; y_t = \begin{bmatrix} I_{PH} \\ T_6 \end{bmatrix}$$

The resistive portion variable and the conductive portion variable of each constitutive component such as the motor or the pump $[P_r]$, $[G_c]$ respectively, should be identified because they are the heart of the Jacobean matrix (as illustrated by Eq. (8)). The other variables $[X_n]$, $[y_r]$ and $[y_a]$ are the sufficient variables needed to characterize the system.

b) Ventilator load torque

This load consists of a dynamic torque T_5 and a static torque T_6 and is given by:

$$T_5 = b_f \omega_5^{c_f} \qquad T_6 = a_f \tag{17}$$

where:

ω_5 , T_5 : Input speed and torque to the centrifugal pump (at edge 5),
a_f : Static torque constant
b_f : Dynamic torque constant
c_f : C factor

The schematic diagram and system graph are shown in Fig. 2.

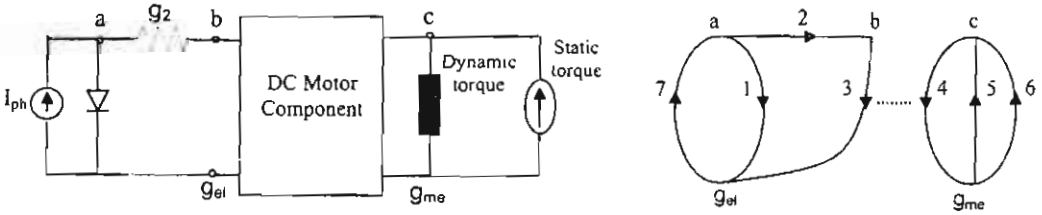

a- Schematic diagram b- System graph

Fig. 2 Schematic diagram and system graph of ventilator load powered by SCA generator

The ***incident matrix*** of this system is:

$$A = \begin{array}{c} \\ a \\ b \\ c \end{array} \begin{array}{c} \begin{array}{ccccccc} A_a & & A_c & & & A_r & A_t \end{array} \\ \begin{array}{ccccccc} 1 & 1 & 2 & 4 & 5 & 3 & 6 & 7 \end{array} \\ \left[\begin{array}{ccccccc} \cdots & 1 & 1 & 0 & 0 & 0 & 0 & -1 \\ \cdots & 0 & -1 & 0 & 0 & 1 & 0 & 0 \\ \cdots & 0 & 0 & 1 & -1 & 0 & -1 & 0 \end{array}\right] \end{array}$$

The ***variables*** required to solve the NRT MN system of equations are:

$$P_r=[V_1] \;:\; G_c=\begin{bmatrix} I_1 \\ I_2 \\ T_1 \end{bmatrix} \;:\; X_n=\begin{bmatrix} V_a \\ V_b \\ \omega_s \end{bmatrix} \;:y_r=[I_1] \;:\; y_1=\begin{bmatrix} I_{FH} \\ T_6 \end{bmatrix}$$

c- Centrifugal pump load

The centrifugal pump is the most popular type used in a PV-pumping system. The motor converts the electrical energy into mechanical energy. The pump converts mechanical energy into hydraulic energy with static head. The terminal equations to represent the operation of the pump can by given by:

$$\omega_5=\omega_{ref}\sqrt{\frac{H_6}{a_{sT}}} \qquad Q_6=\frac{\eta\,\omega_5 T_5}{\rho g H_6} \tag{18}$$

where:
- H_6 Rated head, m
- Q_6 Rated flow charge, liter/min
- η Pump efficiency, %
- p Fluid Density, KG/m3
- g Gravitational constant
- a_{sT} Static a factor

The pictorial representation, schematic diagram and system graph are shown in Fig. 3.

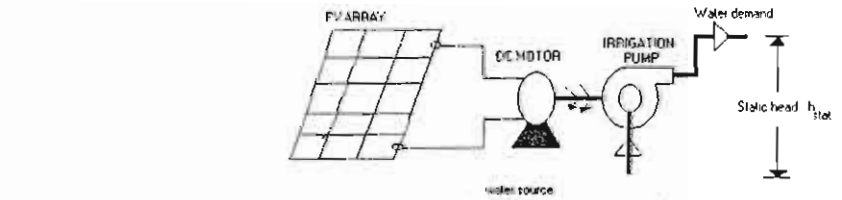

a- Pictorial representation

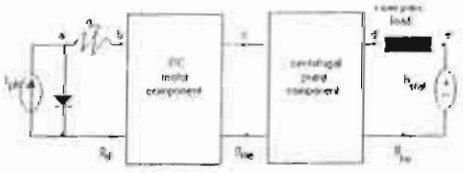

b- Schematic diagram:

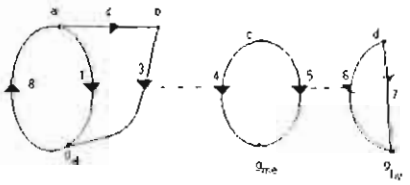

c- System graph

Fig. 3 Pictorial representation, schematic diagram and system graph of centrifugal pump powered by SCA generator

The ***incident matrix*** of this system is:

$$A = \begin{array}{c} \\ a \\ b \\ c \\ d \end{array} \begin{array}{c} \begin{array}{cccccccc} A_a & & A_c & & & A_r & & A_l \end{array} \\ \begin{array}{cccccccc} 7 & 1 & 2 & 4 & 6 & 3 & 5 & 8 \end{array} \\ \left[\begin{array}{c|ccccc|cc} 0 & 1 & 1 & 0 & 0 & 0 & 0 & -1 \\ 0 & 0 & -1 & 0 & 0 & 1 & 0 & 0 \\ 0 & 0 & 0 & 1 & 0 & 0 & 1 & 0 \\ 1 & 0 & 0 & 0 & 1 & 0 & 0 & 0 \end{array}\right] \end{array}$$

The ***variables*** required to solve the NRT MN system of equations are:

$$[P_r]=\begin{bmatrix} V_3 \\ \omega_5 \end{bmatrix};\ [G_c]=\begin{bmatrix} I_1 \\ I_2 \\ T_4 \\ Q_6 \end{bmatrix};\ [X]=\begin{bmatrix} V_a \\ V_b \\ \omega_c \\ h_d \end{bmatrix};\ [X_s]=[h_{state}];\ [Y_r]=\begin{bmatrix} I_3 \\ T_5 \end{bmatrix};\ [Y_a]=[Q_7];\ [Y_t]=[I_{Ph}]$$

4- ANALYSIS OF LOAD MATCHING WITH DIFFERENT MOTOR TYPES USING GTM APPROACH

The quality of load matching for PVPS is a measure of performance quality and degree of the solar cell utilization efficiency. In good matched systems the operation of the load line is close to maximum power line. In this paper the quality of load matching, Q_l is defined as the area under the mechanical load curve with respect to the maximum power line curve. Nine case studies are presented in this section. For each case study, the system components are modeled using GTM approach. Then they are converted to NR MNT and NR R matrices and numerically solved to get (V, I, T, ω) which are sufficient to characterize the system. These parameters are then used to compute the electrical output power of SCA generator, the mechanical output power of the dc motors and the system efficiency and utilization. A computer program is developed to solve these equations numerically using MATLAB 6. The motor, load and SCA generator data used for this study are given in the Appendix.

Following are the final forms of NR MNT and NR R matrices, the input parameter used for each case study, and the results obtained after applying the computer program. Tables 1-3 illustrate the output results, whereas, Figs. 4 -9 show the characteristics and the utilization curve for different case studies.

4-1 A Series Motor Connected to Different Load Types

4.1.1 Constant load

Newton Raphson Mixed Nodal Tableau [NR MNT] & [NR R]

$$\begin{bmatrix} \frac{I_o}{a}e^{\frac{V_a^k}{a}}+g & -g & 0 & 0 \\ g & g & 0 & 1 \\ 0 & 0 & B & -2M_{af}I_3^k \\ 0 & 1 & -M_{af}I_3^k & -R_a-M_{af}\omega_c \end{bmatrix}\begin{bmatrix} V_a^{k+1} \\ V_b^{k+1} \\ \omega_c^{k+1} \\ I_3^{k+1} \end{bmatrix}=\begin{bmatrix} I_{PH}+I_o+e^{\frac{V_a^k}{a}}(\frac{V_a^k}{a}-1) \\ 0 \\ T_L-M_{af}(I_3^k)^2 \\ -M_{af}I_3^k\omega_c^k \end{bmatrix}$$

Table (1-a) Parameters of a series motor connected to a constant load

	100 %	90%	80%	70%	60%
V_a, Volt	154.1195	147.3917	138.064	122.768	80.5671
V_b, Volt	146.7197	140.014	130.6996	115.473	73.418
ω_c, rad/sec	232.0414	220.7005	204.8	178.6588	104.493
I_3, Amp.	8.222	8.1893	8.1549	8.098	7.9344
T, N.m	4.56	4.52	4.489	4.42	4.24

Table (1-b) Results of a series motor connected to a constant load

	100 %	90%	80%	70%	60%
P_{elec}, Watt	1206.3	1146.57	1065.85	935.1	582.53
P_{mech}, Watt	1058.1	997.56	919.35	789.67	443
P_{max}, Watt	1400	1245	1090.76	937.588	785.97
M %	86.16	92.1	97.71	99.73	74.11
H%	87.71	87	86.25	84.45	76.05

4.1.2 Ventilator load

Newton Raphson Mixed Nodal Tableau [NR MNT] & [NR R]

$$\begin{bmatrix} \frac{I_o}{a}e^{\frac{V_a^k}{a}}+g & -g & 0 & 0 \\ -g & g & 0 & 1 \\ 0 & 0 & B+b_f c_f(\omega_c^k)^{c_f-1} & -2M_{af}I_3^k \\ 0 & 1 & -M_{af}I_3^k & -R_a-M_{af}\omega_c \end{bmatrix} \begin{bmatrix} V_a^{k+1} \\ V_b^{k+1} \\ \omega_c^{k+1} \\ I_3^{k+1} \end{bmatrix} = \begin{bmatrix} I_{PH}+I_o+I_o e^{\frac{V_a^k}{a}}(\frac{V_a^k}{a}-1) \\ 0 \\ a_f+(b_f(c_f-1)\omega_c^{c_f})-M_{af}(I_3^k)^2 \\ -M_{af}I_3^k\omega_c^k \end{bmatrix}$$

Table (2-a) Parameters of a series motor connected to a ventilator load

	100 %	90%	80%	70%	60%	50%	40%	30%	20%
V_a	150.06	143.235	134.37	122.28	105.171	82.456	57.898	36.327	19.694
V_b	141.89	135.266	126.673	114.95	98.422	76.55	53.069	32.674	17.250
ω_c	199.285	193.982	186.925	176.94	162.04	140.48	114.064	86.674	61.624
I_3	9.066	8.845	8.549	8.128	7.49	6.56	5.366	4.0551	2.7125
T	5.55	5.28	4.93	4.46	3.76	2.9	1.944	1.109	0.4966

Table (2-b) Results of a series motor connected to a ventilator load

	100 %	90%	80%	70%	60%	50%	40%	30%	20%
P_{max}	1400	1245	1090.76	937.59	785.97	636.57	490.3	348.56	213.67
P_{elect}	1286.3	1196.36	1082.93	934.3	737.18	502.173	284.78	132.49	46.79
P_{mech}	1106.03	1024.22	921.54	789.15	609.27	407.39	221.74	96.12	30.6
μ %	91.88	96.09	99.28	99.65	93.79	78.88	58.12	38.01	21.9
η%	85.98	85.61	85.09	84.45	82.65	78.88	77.86	72.55	65.38

4.1.3 Centrifugal pump load

Newton Raphson Mixed Nodal Tableau [NR MNT] & [NR R]

$$\begin{bmatrix} \frac{I_0}{a}e^{V_a^k/a}+g & -g & 0 & 0 & 0 & 0 & 0 \\ -g & g & 0 & 0 & 1 & 0 & 0 \\ 0 & 0 & B & 0 & -2M_{af}I_3^k & 1 & 0 \\ 0 & 0 & 0 & -\frac{\eta\omega_c^k\tau_5^k}{\rho g(h_d^k)^2} & 0 & \frac{\eta\omega_c^k}{\rho g h_d^k} & 1 \\ 0 & 1 & -M_{af}I_3^k & 0 & -R_a-M_{af}\omega_c^k & 0 & 0 \\ 0 & 0 & 1 & -\frac{\omega_{ref}}{2\sqrt{a_{st}*h_d^k}} & 0 & 0 & 0 \\ & 0 & 0 & 1 & 0 & 0 & 0 \end{bmatrix} * \begin{bmatrix} V_a^{k+1} \\ V_b^{k+1} \\ \omega_c^{k+1} \\ h_d^{k+1} \\ I_3^{k+1} \\ T_5^{k+1} \\ Q_7^{k+1} \end{bmatrix} =$$

$$\begin{bmatrix} I_{ph}-I_0e^{V_a^k/a}(1-\frac{V_a^k}{a})+I_0 \\ 0 \\ -M_{af}(I_3^k)^2 \\ -\frac{\eta\omega_c^k\tau_5^k}{\rho g h_d^k} \\ -M_{af}I_3^k\omega_c^k \\ \omega_{ref}\sqrt{\frac{h_d^k}{a_{st}}}-\frac{\omega_{ref}h_d^k}{2\sqrt{a_{st}*h_d^k}} \\ H_{static} \end{bmatrix}$$

Table (3-a) Parameters of a series motor connected to a centrifugal pump load

	100%	90%	80%	70%	60%	50%	40%	30%	20%
V_a	148	140	130	117	99	75	48.9	28.6	10.4
V_b	140	132	122	109	91.9	68.9	44.1	25.1	8.03
ω_c	194	184	174	158	142	121	88.1	60	11
h_d	57.7	51.6	46.4	38.5	30.9	22.5	11.9	5.5	0.2
I_3	9.15	9.05	8.75	8.45	7.8	6.65	5.4	4.01	2.72
T_5	5.65	5.53	5.16	4.82	4.1	2.98	1.97	1.09	0.5
Q_7	116	120	119	122	115	98.5	89.3	72	189

Table (3-b) Results of a series motor connected to a centrifugal pump load

	100%	90%	80%	70%	60%	50%	40%	30%	20%
P_{max}	1400	1245	1090.7	937.6	785.97	636.57	490.3	348.56	213.67
P_{elect}	1281	1195	1067	921	717	458.2	238	100.4	21.7
P_{mech}	1096	1017	897.8	761.6	582.2	360.6	173.6	65.4	5.5
P_{hyd}	602.8	560	493.8	418.9	320.2	198	95.5	36	3
μ %	91.5	96	97.9	98.3	91.2	72	48.5	28.8	10
η%	85.5	92.3	84.1	82.7	81.2	78.7	72.9	65	25.3

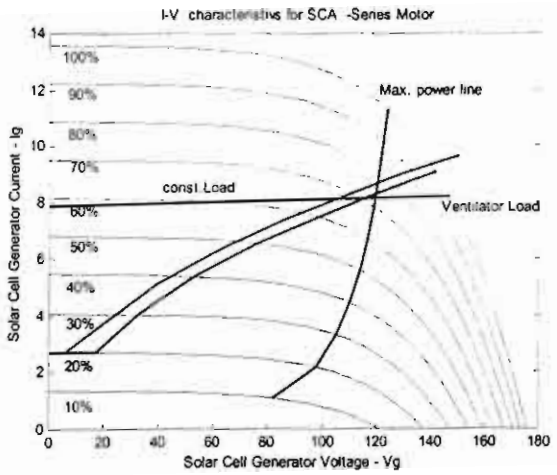

Fig. 4 I-V Characteristics for a series motor connected to different load types

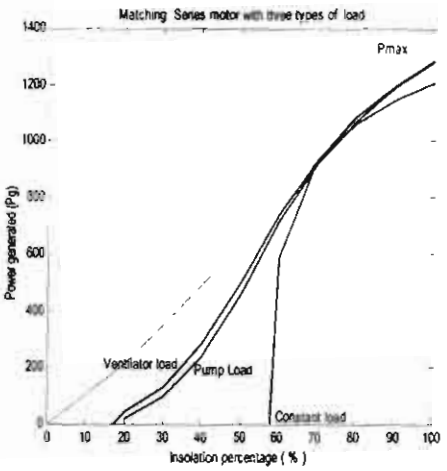

Fig. 5 Utilization curves for a series motor connected to different load types

4.2 A Separately Excited Motor Connected to Different Load Types

4.2.1 Constant load

Newton Raphson Mixed Nodal Tableau [NR MNT] & [NR R]

$$\begin{bmatrix} \frac{I_o}{a}e^{\frac{V_a^k}{a}}+g & -g & 0 & 0 \\ -g & g & 0 & 1 \\ 0 & 0 & B & -c_e \\ 0 & 1 & -c_e & -R_a \end{bmatrix} \begin{bmatrix} V_a^{k+1} \\ V_b^{k+1} \\ \omega_c^{k+1} \\ I_3^{k+1} \end{bmatrix} = \begin{bmatrix} I_{PH}+I_o+e^{\frac{V_a^k}{a}}(\frac{V_a^k}{a}-1) \\ 0 \\ T_L \\ 0 \end{bmatrix}$$

Table (4-a) Parameters of a separately excited motor connected to a constant load

	100 %	90%	80%	70%	60%
V_a	157.7831	152.1904	144.9222	134.5736	116.7616
V_b	151.1982	145.6363	138.408	128.1163	110.4022
ω_c	225.8203	216.9462	205.4135	188.976	160.7305
I_3	7.3092	7.2821	7.2308	7.1748	7.059
T	4.539	4.5222	4.4903	4.4555	4.3836

Table (4-b) Results of a separately excited motor connected to a constant load

	100 %	90%	80%	70%	60%
P_{max}	1400	1245	1090.76	937.588	785.97
P_{elect}	1105.13	1060.5	1000.8	918.59	779.33
P_{mech}	1025	981.07	922.37	841.98	704.57
M%	78.93	85.18	91.75	97.97	99.155
H%	92.75	92.51	92.16	89.8	90.4

4.2.2 Ventilator load

Newton Raphson Mixed Nodal Tableau [NR MNT] & [NR R]:

$$\begin{bmatrix} \frac{I_o}{a}e^{\frac{V_a^k}{a}}+g & -g & 0 & 0 \\ -g & g & 0 & 1 \\ 0 & 0 & B+b_f c_f(\omega_c^k)^{c_f-1} & -c_e \\ 0 & 1 & -c_e & -R_a \end{bmatrix} \begin{bmatrix} V_a^{k+1} \\ V_b^{k+1} \\ \omega_c^{k+1} \\ I_3^{k+1} \end{bmatrix} = \begin{bmatrix} I_{PH}+I_o+I_o e^{\frac{V_a^k}{a}}(\frac{V_a^k}{a}-1) \\ 0 \\ a_f+(b_f(c_f-1)\omega_c^{c_f}) \\ 0 \end{bmatrix}$$

Table (5-a) Parameters of a sep. excited motor connected to a ventilator load

	100 %	90%	80%	70%	60%	50%	40%	30%	20%	10%
V_a	148.819	143.675	137.717	130.74	122.5	112.703	101.025	87.106	70.429	49.835
V_b	140.443	135.765	130.336	123.966	116.415	107.411	96.628	83.707	68.111	48.662
ω_c	203.697	197.415	190.092	181.455	171.157	158.772	143.819	125.68	103.465	75.212
I_3	9.298	8.780	8.193	7.522	6.852	5.874	4.883	3.776	2.5729	1.303
T	5.774	5.4526	5.088	4.671	4.255	3.647	3.033	2.345	1.5977	0.809

Table (5-b) Results of a separately excited motor connected to a ventilator load

	100 %	90%	80%	70%	60%	50%	40%	30%	20%	10%
P_{max}	1400	1245	1090.76	937.588	785.97	636.57	490.3	348.56	213.67	90.3
P_{elect}	1305.82	1192.07	1067.82	932.433	797.67	630.89	471.88	316.08	175.24	63.25
P_{mech}	1176.15	1076.42	967.13	847.57	728.27	579.04	436.146	294.7	165.3	60.85
μ %	93.27	95.75	97.9	99.45	101.49	99.1	96.24	90.68	82.2	70
H%	90.07	90.3	90.57	90.9	91.3	91.78	92.42	93.23	94.32	95.2

4.2.3 Centrifugal pump

Newton Raphson Mixed Nodal Tableau [NR MNT] & [NR R]

$$\begin{bmatrix} \frac{I_0}{a}e^{V_a^k/a}+g & -g & 0 & 0 & 0 & 0 & 0 \\ -g & g & 0 & 0 & 1 & 0 & 0 \\ 0 & 0 & B & 0 & -C_e & 1 & 0 \\ 0 & 0 & 0 & -\frac{\eta\omega_c^k\tau_5^k}{\rho g(h_d^k)^2} & 0 & \frac{\eta\omega_c^k}{\rho g h_d^k} & 1 \\ 0 & 1 & -C_e & 0 & -R_a & 0 & 0 \\ 0 & 0 & 1 & -\frac{\omega_{ref}}{2\sqrt{a_{st}*h_d^k}} & 0 & 0 & 0 \\ & 0 & 0 & 1 & 0 & 0 & 0 \end{bmatrix} * \begin{bmatrix} V_a^{k+1} \\ V_b^{k+1} \\ \omega_c^{k+1} \\ h_d^{k+1} \\ I_3^{k+1} \\ T_5^{k+1} \\ Q_7^{k+1} \end{bmatrix} =$$

$$\begin{bmatrix} I_{ph}-I_0 e^{V_a^k/a}(1-\frac{V_o^k}{a})+I_0 \\ 0 \\ 0 \\ -\frac{\eta\omega_c^k\tau_5^k}{\rho g h_d^k} \\ 0 \\ \omega_{ref}\sqrt{\frac{h_d^k}{a_{st}}}-\frac{\omega_{ref}h_d^k}{2\sqrt{a_{st}*h_d^k}} \\ H_{static} \end{bmatrix}$$

Table (6-a) Parameters of a sep. excited motor connected to a centrifugal pump load

	100%	90%	80%	70%	60%	50%	40%	30%	20%	10%
V_a	146	138	132	122	114	104	90.6	73.5	52.4	16.2
V_b	137	130	124	115	108	98	86	70	50	15
ω_c	197	186	178	166	157	143	126	103	74.2	21
h_d	59.2	53.3	48.8	42	37.6	31.3	24.4	16.4	8.43	0.67
I_3	9.9	9.4	8.8	8.1	7.15	6.1	5.1	3.87	2.62	1.34
T_5	6.14	5.83	5.46	5.03	4.44	3.8	3.17	2.4	1.62	0.83
Q_7	124	125	121	121	113	106	100	93	87.7	159

Table (6-b) Results of a separately excited motor connected to a centrifugal pump load

	100%	90%	80%	70%	60%	50%	40%	30%	20%	10%
P_{max}	1400	1245	1090.7	937.58	785.97	636.57	490.3	348.56	213.67	90.3
P_{elect}	1356	1222	1089	931.5	772.2	543.4	438.6	271	131	20.1
P_{mech}	1209.6	1084.4	971.88	835	697	372.4	272.6	247.2	120.2	17.43
M %	665.28	542.2	534.34	459.25	383.35	204.8	150.1	135.99	66.11	10.5
H%	86.35	98.15	99.1	99.35	98.25	85.63	89.45	77.75	61.3	22.26

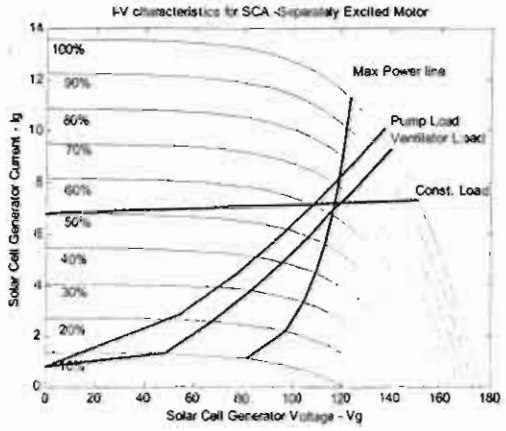

Fig.6 I-V Characteristics for a sep. excited motor connected to different load types

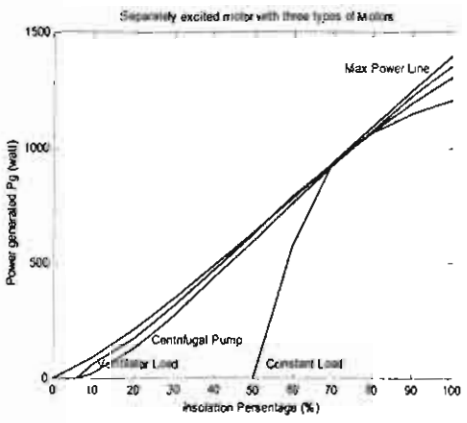

Fig.7 Utilization curves for a sep. excited motor connected to different load types

4.3. A Shunt Motor Connected to Different Load Types

4.3.1 Constant load

Newton Raphson Mixed Nodal Tableau [NR MNT] & [NR R]

$$\begin{bmatrix} \frac{I_o}{a}e^{\frac{V_a^k}{a}}+g & -g & 0 & 0 \\ g & g & 0 & 1 \\ 0 & 0 & B+\frac{M_{af}R_aI_3^2}{(R_a+R_f-M_{af}\omega_4)^2} & \frac{2M_{af}R_aI_3(R_f-M_{af}\omega_4)}{(R_a+R_f-M_{af}\omega_4)^2} \\ 0 & 1 & -\frac{R_fR_aI_3}{(R_a+R_f-M_{af}\omega_4)^2} & \frac{R_fR_a}{(R_a+R_f-M_{af}\omega_4)} \end{bmatrix} \begin{bmatrix} V_a^{k+1} \\ V_b^{k+1} \\ \omega_c^{k+1} \\ I_3^{k+1} \end{bmatrix} =$$

$$\begin{bmatrix} I_{PH}+I_a+e^{\frac{V_a^k}{a}}(\frac{V_a^k}{a}-1) \\ 0 \\ T_L-\frac{M_{af}R_fR_aI_3}{(R_a+R_f-M_{af}\omega_4)^2} \\ -\frac{R_fR_aI_3\omega_4}{(R_a+R_f-M_{af}\omega_4)^2} \end{bmatrix}$$

For the shunt motor connected to constant load torque the motor does not produce sufficient torque to start the system even for the full insolation

4.3.2 Ventilator load

Newton Raphson Mixed Nodal Tableau [NR MNT] & [NR R]

$$\begin{bmatrix} \frac{I_o}{a}e^{\frac{V_a^k}{a}}+g & -g & 0 & 0 \\ g & g & 0 & 1 \\ 0 & 0 & B+\frac{M_{af}R_aI_3^2}{(R_a+R_f-M_{af}\omega_4)^2}+b_fc_f(\omega_c^k)^{c_f-1} & \frac{2M_{af}R_aI_3(R_f-M_{af}\omega_4)}{(R_a+R_f-M_{af}\omega_4)^2} \\ 0 & 1 & -\frac{R_fR_aI_3}{(R_a+R_f-M_{af}\omega_4)^2} & -\frac{R_fR_a}{(R_a+R_f-M_{af}\omega_4)} \end{bmatrix} \begin{bmatrix} V_a^{k+1} \\ V_b^{k+1} \\ \omega_c^{k+1} \\ I_3^{k+1} \end{bmatrix} =$$

$$\begin{bmatrix} I_{PH}+I_o+e^{\frac{V_a^k}{a}}(\frac{V_a^k}{a}-1) \\ 0 \\ T_f-\frac{M_{af}R_aR_fI_3}{(R_a+R_f-M_{af}\omega_4)^2}+(b_f(c_f-1)\omega_c^{c_f}) \\ -\frac{R_fR_aI_3\omega_4}{(R_a+R_f-M_{af}\omega_4)^2} \end{bmatrix}$$

Table (7-a) Parameters of a shunt motor connected to a ventilator load

	100 %	90%	80%	70%	60%
V_a	163.7	156.9	37.2	31	25.77
V_b	157	150	27.5	22.5	18.5
ω_c	181.3	180.1	81.78	73.36	68.5
I_3	7.4	7.7	10.75	9.45	8.08
T	5.64	5.506	1.507	1.085	0.763

Table (7-b) Results of a shunt motor connected to a ventilator load

	100 %	90%	80%	70%	60%
P_{max}	1400	1245	1090.76	937.6	785.97
P_{elect}	1160	1155	295.6	212.6	149.48
P_{mech}	1023.3	992.3	123.3	79.6	52.3
M %	96.5	85.9	27.1	22.7	18.5
H%	88.2	86	41.7	37.41	35

4.3.3 Centrifugal pump

Newton Raphson Mixed Nodal Tableau [NR MNT] & [NR R]

$$\begin{bmatrix} \frac{I_0}{a}e^{V_a^k/a}+g & -g & 0 & 0 & 0 & 0 & 0 \\ -g & g & 0 & 0 & 1 & 0 & 0 \\ 0 & 0 & B+\frac{M_{af}R_aI_3^2}{(R_a+R_f-M_{af}\omega_4)^2} & 0 & \frac{2M_{af}R_aI_3(R_f-M_{af}\omega_4)}{(R_a+R_f-M_{af}\omega_4)^2} & 1 & 0 \\ 0 & 0 & 0 & -\frac{\eta\omega_c^k r_5^k}{\rho g(h_d^k)^2} & 0 & \frac{\eta\omega_c^k}{\rho g h_d^k} & 1 \\ 0 & 1 & \frac{R_fR_aI_3}{(R_a+R_f-M_{af}\omega_4)^2} & 0 & \frac{R_fR_a}{(R_a+R_f-M_{af}\omega_4)} & 0 & 0 \\ 0 & 0 & 1 & -\frac{\omega_{ref}}{2\sqrt{a_H * h_d^k}} & 0 & 0 & 0 \\ 0 & 0 & 0 & 1 & 0 & 0 & 0 \end{bmatrix} * \begin{bmatrix} V_a^{k+1} \\ V_b^{k+1} \\ \omega_c^{k+1} \\ h_d^{k+1} \\ I_3^{k+1} \\ T_5^{k+1} \\ Q_7^{k+1} \end{bmatrix} =$$

$$\begin{bmatrix} I_{ph}-I_0e^{V_a^k/a}(1-\frac{V_a^k}{a})+I_0 \\ 0 \\ -\frac{M_{af}R_fR_aI_3}{(R_a+R_f-M_{af}\omega_4)^2} \\ -\frac{\eta\omega_c^k r_5^k}{\rho g h_d^k} \\ \frac{R_fR_aI_3\omega_4}{(R_a+R_f-M_{af}\omega_4)^2} \\ \omega_{ref}\sqrt{\frac{h_d^k}{a_H}}-\frac{\omega_{ref}h_d^k}{2\sqrt{a_H * h_d^k}} \\ H_{static} \end{bmatrix}$$

Table (8-a) Parameters of a shunt motor connected to a centrifugal pump load

	100%	90%	80%	70%	60%
V_a	162.7	154.9	38.2	32.24	25.77
V_b	157	150	27.5	22.5	18.5
ω_c	181.3	180.1	81.78	73.36	68.5
h_d	67.7	53	46.4	38.5	30.9
I_3	7.6	7.8	10.35	9.4	8.08
T_5	5.84	5.65	1.67	1.01	0.763
Q_7	110	121	102	118	121

Table (8-b) Results of a shunt motor connected to a centrifugal pump load

	100%	90%	80%	70%	60%
P_{max}	1400	1245	1090.76	937.6%	785.97
P_{elect}	1158	1145	292.6	210.6	149.48
P_{mech}	1020.3	991.3	122.3	81.6	52.3
P_{hyd}	590	545.215	71.1	47.14	26.15
μ %	96.1	83.9	25.1	21.7	18.5
η%	87.2	85.8	41.4	37.21	35

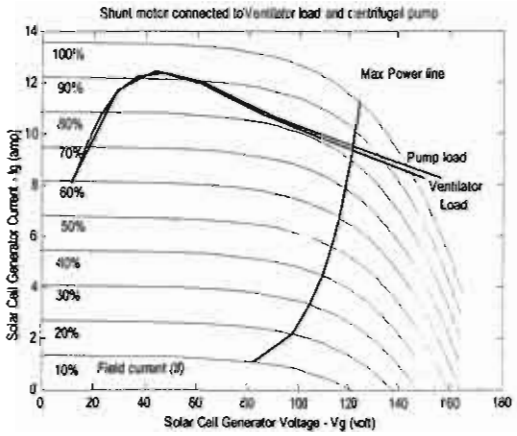

Fig.8 I-V characteristics of a shunt motor connected to different load types

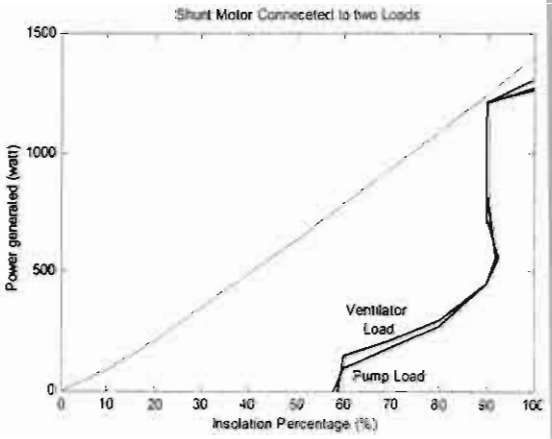

Fig. 9 Utilization curves for a shunt motor connected to different load types

4-4 COMPARISON BETWEEN CASE STUDIES

A comparison between the nine case studies is presented in Table 9 and it shows that:

- The separately excited motor is the appropriate type for a different mechanical load types. Its efficiency and matching quality are better than other motors.
- Separately excited motor coupled to a ventilator load type is found to be the most suitable combination for SCA generator. The utilization of SCA output energy is 96.07% of its maximum output power.
- It is not preferable to use shunt motors with constant mechanical loads. However, the SCA generator can produce sufficient torque to start up the shunt motor to

supply both ventilator and centrifugal pump loads (at 59.6%, and 59% of insolation level respectively).

Table 9-a Constant load

Motor type	Start up insolation level	Matching quality	efficiency
Series motor	57.94%	62.73%	89.96%
Separately motor	49.68%	65.84%	92.05%
Shunt motor	-----	—	----

Table 9-b Ventilator load

Motor type	Start up insolation level	Matching quality	Efficiency
Series motor	19.99%	83.84%	84.17%
Separately motor	5.9%	96.07%	92%
Shunt Motor	59.6%	32.25%	81%

Table 9-c Centrifugal pump

Motor Type	Start up insolation level	Matching quality	Efficiency
Series motor	20%	81.73%	82.75%
Separately motor	6%	93.5%	90.7%
Shunt Motor	59%	29.66%	81.08%

5- CONCLUSION

- The systematic mathematical methodology known as Graph Theoretic Modeling (GTM) was presented in details.
- The GTM technique has been applied to PVPS composed of different dc-motor types (series, separately excited and shunt motors) connected to different load types (constant, ventilator and pump loads) supplied by a SCA generator.
- A computer program using MATLAB 6 was developed to numerically solve the system matrix equations.
- The quality of load matching for each case was investigated as a measure of performance and system utilization efficiency.
- A comparison between different case studies was introduced to indicate the appropriate motor type for each load.
- Applying the GTM technique to PV systems results in many advantages:
  - GTM methodology is global and flexible enough to include linear or nonlinear components and replace them with a stamp.
  - GTM analyzes electrical and mechanical characteristics for combined PV-dc motor in addition to hydraulic characteristics in case of centrifugal pump.
  - GTM technique is a general integral promising methodology capable of providing PVPS with ready simulated stamps for any component.
  - GTM technique as a mathematical methodology can be used as a measure of matching quality, which reflect the performance of the system and exhibit the appropriate load connected to a dc motor powered by SCA generator.

- The paper presents a method for modeling SCA generator, different types of dc-motors and various mechanical loads. It provides an evaluation for any motor type connected to a mechanical load powered by a stand-alone PV power system.

6- REFERENCES

1. J. Appelbaum and J. Bany, "*Performance Analysis of DC Motor Photovoltaic Converter System*", Solar Energy, Vol.22, PP.439 – 445, 1979.
2. J. Appelbaum, "*Performance Analysis of DC Motor Converter System: Series and Shunt Excited Motor*" , Solar Energy, vol.27, PP. 23 – 30 , 1981.
3. J. Appelbaum, "*Starting and Steady State Characteristics of DC Motor Powered by Solar Cell Generator*", IEEE Transactions on Energy Conversion, Vol. EC –1, No.1, PP. 17 –25, March 1986.
4. F. Hilmer, A. Ratka and O. Melsheimer, "*An Investigation of Directly Coupled Photovoltaic Pumping System Connected to a large Absorber Filed*" Solar Energy Vol.61, NO.2, PP.65–76, 1997
5. J. Eckstein, "*Detailed Modeling of Photovoltaic System Components*", M.Sc. thesis, Mechanical Engineering Dept., University of Wisconsin–Madison, 1990.
6. A.M. AL–Ibrahim, "*Optimal Selection of Direct Coupled Photovoltaic Pumping System in Solar Domestic Hot Water Systems*" Ph.D. thesis, Mechanical Engineering Dept., University of Wisconsin–Madison, 1996.
7. Q. KOU, "*A Method of Estimation Long–Term Performance of PV Pumping System*" MSc Thesis Wisconsin –Madison University, 1996.
8. M. Kolhe and J.C. Joshi, "*Performance Analysis of Directly Coupled Photovoltaic Electro-Mechanical Systems*", Proceeding Institution Mechanical Engineering, Vol. 216, PP. 453-462, 2002.
9. A. M. Al-Ibrahim, "*Design Procedure for Selecting an Optimum Photovoltaic Pumping System in Solar Systems*", Solar Energy, Vol. 64 Issue 4-6, pp. 227-240, 1998.
10. H. Koenig, Y. Tokad, and H. Kesavan, "*Analysis of Discrete Physical Systems*", McGraw-Hill, New York 1967
11. S. Gupta and M. Chandrashkar, "*A Unified Approach to Modeling Photovoltaic Powered Systems*", Solar Energy, Vol.55, NO.4, PP.267 –285, 1995.

APPENDIX

Parameter Values

Component	Symbol	Nomenclature	Value
PV Cell	I_0	Reverse Saturation current	$8.1e^{-3}$ A
	I_{ph}	Cell photocurrent	0.756 A
	R_s	Cell series resistance	0.05 ohm
	σ	Thermal voltage (A=KT/q)	1/13.68 1/Volt
	K	Botzman constant	
	T	Absolute temperature	300 Kelvin
	q	Electron charge	$1.6\ e^{-19}$ coulomb
Output Motor Data	V	Terminal voltage	120 Volt (rated)
	I_a	Armature current	9.2 A (rated)
	ω	Shaft speed	157.1 rad/sec
	T_m	Electromagnetic torque	5.7 N.m
	A	Toque constant of rotational losses	0.2 N.m
	B	Viscous Torque constant of rotational losses	$2.387e^{-3}$ N.m /rad/s
Series Motor	R_a	Combined field and armature resistance	2.2 ohm
	M_{af}	Mutual inductance between field and armature	$6.75e^{-2}$ H
Sep. Excited Motor	R_a	Armature resistance	1.5 ohm
	C_f	Flux coefficient	0.621 V/rad/sec
Shunt Motor	M_{af}	Mutual inductance between field and armature	0.518 H
	R_a	Armature resistance	1.5 ohm
	R_f	Field resistance	100 ohm
Constant Load	T_l	Load torque	4.0 N.m
Ventilator Load	a_f	Static torque constant	$3.0\ e^{-1}$ N.m
	b_f	Dynamic torque constant	$3.9\ e^{-4}$
	c_f	C factor	1.8
Centrifugal Pump	H	Rated head. m	37.795
	Q	Rated flow charge, liter/min	80
	η	Pump efficiency, %	55
	ρ	Fluid Density, KG/m3	1000
	g	Gravitational constant	9.8
	a_{ST}	Static a factor	37.795